Luminescent Silicon Nanoparticles Capped by Conductive Polyaniline through the Self-Assembly Method

Z. F. Li, M. T. Swihart, and E. Ruckenstein*

Department of Chemical and Biological Engineering, State University of New York at Buffalo, Buffalo, New York 14260

Received October 9, 2003. In Final Form: December 11, 2003

Graft polymerization has been used, for the first time, to prepare a dense conductive polymer coating on free-standing luminescent silicon nanoparticles. The silicon nanoparticles maintained their photoluminescence and crystallinity after surface modification. The nanoparticles were first surface hydroxylated and then reacted with (3-bromopropyl)trichlorosilane to form a dense bromopropylsilane monolayer. This was further reacted with aniline, which displaced the bromine atoms. The surface-bound aniline molecules were then used as active sites for the graft polymerization of polyaniline (PANI). The composition, structure, morphology, and other physical properties of the PANI-capped Si nanoparticles were examined by X-ray photoelectron spectroscopy, Fourier transform infrared spectroscopy, X-ray diffraction, and transmission electron microscopy. The silane self-assembled monolayer effectively protected the silicon particles against photoluminescence quenching and degradation in basic solutions that rapidly quench the photoluminescence of unprotected particles. The PANI coating further enhanced this protection, even in its nonconducting emeraldine base state. The electrical conductivity of the HCl-doped (emeraldine salt) PANI-capped Si nanocomposite exceeded 10^{-2} S/cm, which is 6 orders of magnitude higher than that of the bare Si nanoparticles. However, there was negligible change in the photoluminescence spectrum or lifetime upon addition of the PANI layer, suggesting that the charge carriers responsible for the luminescence remained confined within the Si nanoparticles.

Introduction

Nanoparticles of many materials have received great attention lately, as researchers have become increasingly aware that reducing the size of materials to the nanometer scale can change their properties in fundamental ways, thus generating attractive electronic, optical, magnetic, and/or catalytic properties associated with their nanoscale or quantum-scale dimensions.[1] Following the discovery in 1990 of visible red light emission upon UV excitation of electrochemically etched nanoporous silicon by Canham and co-workers,[2] a great deal of research has been performed on producing nanosized Si with visible photoluminescence and on characterization of its structure and optoelectronic properties.[3−8] This luminescence from nanosized Si has been attributed to radiative recombination of carriers confined in Si nanoparticles, and its color can be modified from blue to red by changing the nanoparticle size. One benefit of exploiting the optical properties of silicon nanoparticles over the other materials is the potential of silicon nanoparticles to be integrated within existing silicon technologies in order to create nanoscale optoelectronic devices. These applications include their use as chemical sensors,[9] optoelectronic devices,[10] electroluminescent displays,[11] photodetectors,[12] and as a lasing material for photopumped tunable lasers.[13] In addition, the silicon nanoparticles' good biocompatibility,[14] high photoluminescence quantum efficiency,[15] and stability against photobleaching,[16] make them an ideal candidate for replacing fluorescent dyes in many biological assays and fluorescence imaging techniques.

Because of the relative ease of preparing luminescent porous silicon films by etching silicon wafers, there have been many studies of surface modification of porous silicon films by various organic compounds ranging from alkyl chains to macromolecules, to develop new building blocks for optical, electrical, and biomedical applications. This includes free radical initiation to form alkyl monolayers,[17,18] derivatization with alcohols through electrochemical and thermal reactions,[19] derivatization with halogens,[20] photoelectrochemical esterification reactions with car-

* Corresponding author: tel, (1-716) 645-2911, ext 2214; fax, (1-716) 645-3822; e-mail, feaeliru@acsu.buffalo.edu (E. Ruckenstein).

(1) (a) Wegner, G. *Angew. Chem., Int. Ed. Engl.* **1981**, *20*, 361. (b) Niemeyer, C. M. *Angew. Chem., Int. Ed.* **2001**, *40*, 4128. (c) Remacle, F.; Levine, R. D. *Chem. Phys. Chem.* **2001**, *2*, 20.
(2) Canham, L. T. *Appl. Phys. Lett.* **1990**, *57*, 1046.
(3) Heath, J. R. *Science* **1992**, *258*, 1131.
(4) Lu, Z. H.; Lockwood, D. J.; Baribeau, J.-M. *Nature* (*London*) **1995**, *378*, 258.
(5) Vinciguerra, V.; Franzo, G.; Priolo, F.; Iacona, F.; Spinella,C. *J. Appl. Phys.* **2000**, *87*, 8165.
(6) Wakayama, Y.; Tagami, T.; Inokuma, T.; Hasegawa, S.; Tanaka, Sh. *Res. Dev. Cryst. Growth* **1999**, *1*, 83.
(7) Rinnert, H.; Vergnat, M.; Marchal, G. *Mater. Sci. Eng., B* **2000**, *69−70*, 484.
(8) Huisken, F.; Kohn, B. *Appl. Phys. Lett.* **1999**, *74*, 3776.
(9) (a) Lin, V. S. Y.; Motesharei, K.; Dancil, K. P. S.; Sailor, M. J.; Ghadiri, M. R. *Science* **1997**, *278*, 840. (b) Harper, J.; Sailor, M. J. *Anal. Chem.* **1996**, *68*, 3713.
(10) Hamilton, B. *Semicond. Sci. Technol.* **1995**, *10*, 1187.
(11) Doan, V. V.; Sailor, M. J. *Science* **1992**, *256*, 1791.
(12) Sailor, M. J.; Heinrich, J. L.; Lauerhaas, J. M. *Semiconductor Nanoclusters*; Kamat, P. V., Meisel, D., Eds.; Elsevier Science: New York, 1996; Vol. 103.
(13) Canham, L. T. *Appl. Phys. Lett.* **1993**, *63*, 337.
(14) Yoshinobu, T.; Ecken, H.; Ismail, A. B. M.; Iwasaki, H.; Luth, H.; Schoning, M. J. *Electrochim. Acta.* **2001**, *47*, 259.
(15) Delerue, C.; Allan, G.; Lannoo, M. *Phys. Rev. B* **1993**, *48*, 11024.
(16) Bruchez, M., Jr.; Moronne, M.; Gin, P.; Weiss, S.; Alivisatos, A. P. *Science* **1998**, *281*, 2013.
(17) (a) Buriak, J. M.; Stewart, M. P.; Geders, T. W.; Allen, M. J.; Choi, H. C.; Smith, J.; Raftery, D.; Canham, L. T. *J. Am. Chem. Soc.* **1999**. *121*, 11491. (b) Buriak, J. M. *Chem. Rev.* **2002**, *102*, 1271.
(18) (a) Linford, M. R.; Chidsey, C. E. *J. Am. Chem. Soc.* **1993**, *115*, 12631. (b) Linford, M. R.; Fenter, P.; Eisenberger, P. M.; Chidsey, C. E. *J. Am. Chem. Soc.* **1995**, *117*, 3145.
(19) (a) Warntjes, M.; Vieillard, C.; Ozanam, F.; Chazalviel, J.-N. *J. Electrochem. Soc.* **1995**, *142*, 4138. (b) Krawiec, B. S.; Cassagneau, T.; Fendler, J. H. *J. Phys. Chem. B* **1999**, *103*, 9524.
(20) Lauerhaas, J. M.; Sailor, M. J. *Science* **1993**, *261*, 1567.

10.1021/la0358926 CCC: $27.50
Published on Web 01/20/2004

boxylic acids and with alcohols,[21] and reactions with chlorosilanes.[22] In addition, modification of the porous silicon film by polymer deposition was also achieved to improve its functionality for use in sensors, electroluminescent devices, and other hybrid devices.[23−27]

Several methods have been developed to produce free-standing silicon nanoparticles that are nonporous and free from a substrate. These include ultrasonic dispersion of porous silicon,[28] solution synthesis,[29] gas-phase decomposition of silanes,[30] laser-vaporization controlled condensation,[31] organosilane decomposition in supercritical organic solvents,[32] and laser-driven decomposition of silane.[33] However, the above methods cannot produce more than a few milligrams per day of luminescent Si nanoparticles that are free from a substrate. This has hindered research on these free-standing silicon nanoparticles, and relatively few studies have been presented on surface functionalization of free-standing silicon nanoparticles with polymers or other organic moieties. Recently, free silicon nanoarticles that exhibit bright visible photoluminescence have been successfully produced in macroscopic quantities (hundreds of milligrams per day).[34] These are prepared in a two-step process in which silicon nanoparticles are synthesized by CO_2 laser heating of SiH_4-H_2-He mixtures followed by etching of the nanoparticles with a hydrofluoric acid/nitric acid mixture to reduce their size and passivate their surface. This technique is a valuable tool for producing large amounts of free luminescent silicon nanoparticles in a controlled and reproducible way. The availability of free silicon nanoparticles prepared by the above method allows us to prepare and study free-standing polymer/Si nanocomposites that can potentially exhibit unique optical, chemical, and mechanical properties.

Among the methods to produce nanocomposites, modification and functionalization of nanoparticle surfaces have become an area of intense interest, since one of the requirements for realizing functional nanomaterials is the availability of suitably modified nanoparticle building blocks.[35] Recently, nanocomposites of conductive polymers and inorganic particles have received much attention.[36] As one-dimensional semiconductors, some conductive polymers have the advantage of being easy to process into large-area devices, and their energy gaps and ionization potentials can be tuned by chemical modification of the polymer chains.[37] Among them, polyaniline (PANI) is distinguished by its high electrical conductivity, redox properties, environmental stability, ease of processing, and low cost.[38] It has extensive applications in areas including Li ion batteries,[39] light-emitting devices,[40,41] corrosion protection,[42] radio frequency and microwave absorption,[43] and electromagnetic interference shielding and antistatic films and coatings.[44] Several types of inorganic nanoparticles have been encapsulated in conductive polymers, and such nanocomposites have shown various interesting characteristics, particularly in their dielectric properties, energy storage capability, catalytic activity, and magnetic susceptibility.[45]

The coating of polyaniline onto silicon nanoparticles is of particular interest because of potential applications in optical emitters and detectors. Because of its large work function, PANI has been used as a hole-transporting material in polymeric LEDs.[46] The work function of PANI in its emeraldine base and emeraldine salt forms has been estimated for different samples and by various methods to be from 4.3 to 4.7 eV,[47] about 4.8 eV,[48] or more than 5 eV.[46] In addition, the work function and conductivity of PANI can be changed by varying the counterion used for doping. It appears that work function can be tuned independently of conductivity.[49] The energy band struc-

(21) (a) Lee, E. J.; Ha, J. S.; Sailor, M. J. *J. Am. Chem. Soc.* **1995**, *117*, 8295. (b) Lee, E. J.; Bitner, T. W.; Shane, M. J.; Ha, J. S.; Sailor, M. J. *J. Am. Chem. Soc.* **1996**, *118*, 5375.

(22) Anderson, R. C.; Muller, R. C.; Tobias, C. W. *J. Electrochem. Soc.* **1993**, *140*, 1393.

(23) Bakker, J. W. P.; Arwin, H.; Wang, G.; Jarrendahl, K. *Phys. Status Solidi A* **2003**, *197*, 378.

(24) Nguyen, T. P.; Le Rendu, P.; Cheah, K. W. *Physica E* **2003**, *17*, 664.

(25) Lakehal, M.; Nguyen, T. P.; Le Rendu, P.; Joubert, P.; Destruel, P. *Synth. Met.* **2001**, *121*, 1631.

(26) Moreno, J. D.; Marcos, M. L.; Agullo-Rueda, F.; Guerrero-Lemus, R.; Martin-Palma, R. J.; Martinez-Duart, J. M.; Gonzalez-Velasco, J. *Thin Solid Films* **1999**, *348*, 152.

(27) Monastyrskii, L.; Lesiv, T.; Olenych, I. *Thin Solid Films* **1999**, *344*, 335.

(28) (a) Heinrich, J. L.; Curtis, C. L.; Credo, G. M.; Kavanagh, K. L.; Sailor, M. J. *Science* **1992**, *255*, 66. (b) Bley, R. A.; Kauzlarich, S. M.; Davis, J. E.; Lee, H. W. H. *Chem. Mater.* **1996**, *8*, 1881.

(29) (a) Wilcoxon, J. P.; Samara, G. A.; Provencio, P. N. *Phys. Rev. B* **1999**, *60*, 2704. (b). Mayeri, D.; Phillips, B. L.; Augustine, M. P.; Kauzlarich, S. M. *Chem. Mater.* **2001**, *13*, 765. (c) Bley, R. A.; Kauzlarich, S. M. A *J. Am. Chem. Soc.* **1996**, *118*, 12461 (d) Heath, J. R. *Science* **1992**, *258*, 1131.

(30) (a) Wilson, W. L.; Szajowski, P. J.; Brus, L. *Science* **1993**, *262*, 1242. (b) Ostraat, M. L.; De Blauwe, J. W.; Green, M. L.; Bell, L. D.; Brongersma, M. L.; Casperson, J.; Flagan, R. C.; Atwater, H. A. *Appl. Phys. Lett.* **2001**, *79*, 433. (c) Fojtik, A.; Weller, H.; Fiechter, S.; Henglein, A. *Chem. Phys. Lett.* **1987**, *134*, 477. (d) Littau, K. A.; Szajowshki, P. J.; Muller, A. J.; Kortan, A. R.; Brus, L. E. *J. Phys. Chem.* **1993**, *97*, 1224.

(31) Carlisle, J. A.; Dongol, M.; Germanenko, I. N.; Pithawalla, Y. B.; El-Shall, M. S. *Chem. Phys. Lett.* **2000**, *326*, 335.

(32) (a) English, D. S.; Pell, L. E.; Yu, Z. H.; Barbara, P. F.; Korgel, B. A. *Nano Lett.* **2002**, *2*, 681. (b) Holmes, J. D.; Ziegler, K. J.; Doty, R. C.; Pell, L. E.; Johnston, K. P.; Korgel, B. A. *J. Am. Chem. Soc.* **2001**, *123*, 3743.

(33) Ehbrecht, M.; Ferkel, H.; Smirnov, V. V.; Stelmakh, O.; Zhang, W.; Huisken, F. *Surf. Rev. Lett.* **1996**, *3*, 807. (b) Ehbrecht, M.; Kohn, B.; Huisken, F.; Laguna, M. A.; Paillard, V. *Phys. Rev. B* **1997**, *56*, 6958. (c) Ledoux, G.; Gong, J.; Huisken, F.; Guillois, O.; Reynaud, C. *Appl. Phys. Lett.* **2002**. *80*, 4834.

(34) Li, Xuegeng, He Yuanqing, Talukdar, S. S.; Swihart, M. T. *Langmuir* **2003**, *19*, 8490.

(35) (a) Sailor, M. J.; Lee, M. J. *Adv. Mater.* **1997**, *9*, 78. (b) Kamat P. V. *J Phys. Chem. B* **2002**, *106*, 7729.

(36) (a) Colvin, V. L.; Schlamp, M. C.; Alivisatos, A. P. *Nature* **1994**, *370*, 354. (b) Cassagneau, T.; Mallouk, T. E.; Fendler, J. H. *J. Am. Chem. Soc.* **1998**, *120*, 7848 (c) Gao, M.; Richer, B.; Kirstein, S. *Adv. Mater.* **1997**, *9*, 802. (d) Gangopadhyay, R.; De, A. *Chem. Mater.* **2000**, *12*, 608.

(37) Grem, G.; Leditzky, G.; Ullrich, B.; Leising, G. *Adv. Mater.* **1992**, *4*, 36.(b). Greenham, N. C.; Morratti, S. C.; Bradley, D. D. C.; Friend, R. H.; Holmes, A. B. *Nature* **1993**, *365*, 628.

(38) (a) Singh, R.; Tandon, R. P.; Chandra, S. *J. Appl. Phys.* **1991**, *70*, 243. (b) Joo, J.; Epstein, A. J. *Appl. Phys. Lett.* **1994**, *65*, 2278.

(39) MacDiarmid, A. G.; Kanner, R. B. In *Handbook of Conducting Polymers*; Skotheim, T. A., Ed.; Marcel Dekker: New York,1986; Vol. 1, p 687.

(40) Burroughes, J. H.; Bradley, D. D. C.; Brown, A. R.; Marks, R. N.; Friend, R. H.; Burns, P. L.; Holmes, A. B. *Nature* **1990**, *347*, 539.

(41) (a) Halliday, D. P.; Gray, J. W.; Adams, P. N.; Monkman, A. P. *Synth. Met.* **1999**, *102*, 877. (b) Halliday, D. P.; Holland, E. R.; Eggleston, J. M.; Adams, P. N.; Cox, S. E.; Monkman, A. P. *Thin Solid Films* **1996**, *276*, 299.

(42) Racicot, R.; Brown, R.; Yang, S. C. *Synth. Met.* **1997**, *85*, 1263.

(43) Dhawan, S. K.; Singh, N.; Venkatachalam, S. *Synth. Met.* **2002**, *129*, 261.

(44) Makela, T.; Pienimaa, S.; Taka, T.; Jussila, S.; Isotalo, H. *Synth. Met.* **1997**, *85*, 1335.

(45) (a) Sukeerthi, S.; Contractor, A. Q. *Chem. Mater.* **1998**, *10*, 2412. (b) Flitton, R.; Johal, J.; Maeda, S.; Armes, S. P. *J. Colloid Interface Sci.* **1995**, *173*, 135. (c) Gangopadhyay, G.; De, A. *J. Appl. Phys.* **2000**, *87*, 2363. (d) Cho, G.; Fung, B. M.; Glatzhofer, D. T.; Lee, J. S.; Shul, Y. G. *Langmuir* **2001**, *17*, 456.

(46) Higgins, R. W. T.; Zaidi, N. A.; Monkman, A. P. *Adv. Functional Mater.* **2001**, *11*, 407.

(47) Liess, M.; Chinn, D.; Petelenz, D.; Janata, J. *Thin Solid Films* **1996**, *286*, 252.

(48) Halliday, D. P.; Eggleston, J. M.; Adams, P. N.; Pentland, I. A. Monkman, A. P. *Synth Met.* **1997**, *85*, 1245.

(49) Polk, B. J.; Potje-Kamloth, K.; Josowicz, M.; Janata, J. *J. Phys. Chem. B* **2002**, *106*, 11457.

tures for the different forms of PANI are presented in a paper by Huang and MacDiarmid.[50] For bulk Si, the electron affinity is 4.05 eV and the band gap is 1.12 eV, so the top of the valence band is 5.17 eV below vacuum. This is comparable to, but probably greater than, the PANI work function. In silicon nanoparticles, the band gap widens, but it is not clear how the band alignment will change. Thus, PANI is a reasonable candidate for a hole-transport material for injection of positive charge carriers into Si nanocrystals for hybrid inorganic/organic light-emitting devices. Quantum-dot photodetectors[51] based on photoconductive PANI/silicon nanoparticle nanocomposites are another interesting possiblility. In these, positive charge carriers would be optically excited from the Si nanoparticles into the PANI, increasing the conductivity of the nanocomposite upon illumination.

To construct a highly dense polymer coating on the surface of the nanoparticles, the so-called "grafting from" techniques are preferable to methods that attempt to link existing polymer chains to the surface.[52] In "grafting from" methods, as used here, the small monomer molecules can freely access the active initiation sites and the ends of the growing polymer chains. In linking existing polymer chains to a surface, there is inevitably a steric barrier to incoming polymers imposed by chains that are already attached, and this limits the density of attachments of the polymer chains to the surface.[53] The surface-initiated polymerization in conjunction with a self-assembly (SAM) technique is among the most useful synthetic routes to precisely design and functionalize the surfaces of various solid materials by well-defined polymers and copolymers.[52] A method of surface graft polymerization of aniline on photopatterned self-assembled phenylsilane monolayers to generate well-defined patterns of conductive polyaniline on a planar Si(100) surface was previously reported.[54] This method generated a compact grafted PANI with high edge acuity of the pattern, which provided a new strategy for the generation of a pattern of conductive polymers via graft polymerization. In the present work, we use (3-bromopropyl)trichlorosilane to first form a self-assembled monolayer on the surface of silicon nanoparticles. Then, after functionalization of the SAM monolayer through aniline substitution, further surface oxidative graft polymerization forms a dense layer of polyaniline. This work presents a detailed characterization of conductive polymer coated Si nanoparticles. After this surface modification and acid doping of the PANI, the coated particles exhibit a bulk electrical conductivity near 10^{-2} S/cm. The photoluminescence (PL) of the bare Si nanoparticles can be quenched by exposure to various substances, as has been widely reported for porous silicon. The resulting lack of stability of the PL could limit many applications of this novel material. In contrast, silicon nanoparticles coated with PANI using the self-assembly method are much more robust and maintain their photoluminescence after long exposures to solvents and basic solutions that would otherwise degrade the PL properties. In addition, experiments regarding the electromagnetic interference (EMI) shielding of the PANI grafted Si nanoparticles are also included in the paper to demonstrate the surface conductive effect of grafted PANI. With increasing chip density of transistor electronics, the problem of electromagnetic and radio frequency interference and electrostratic dissipation to avoid electrostratic shock becomes especially acute and sometimes can damage the brittle circuit elements.[55] This first reported grafting of a conductive polymer to silicon nanoparticles shows one way that the polymer and nanoparticle properties can be combined. The graft polymerization strategy used here can also be adapted to other polymers. The ability to prepare these hybrid organic/inorganic nanoparticles will broaden the potential applications of luminescent Si nanoparticles.

Experimental Section

Materials. The chemical reagents, aniline, (3-bromopropyl)-trichlorosilane, and ammonium persulfate were obtained from Aldrich/Sigma and were used as received. The anhydrous toluene was dried over 4 Å molecular sieves prior to use. Other solvents, such as acetone, ethanol, *N*-methylpyrrolidinone (NMP), and hexylamine, as well as other chemicals were of reagent grade and were also purchased from the Aldrich/Sigma Chemical Co. and used as received.

The nanosized (around 3−5 nm) crystalline silicon powder was synthesized as described in detail previously.[34] The particles were generated by laser-induced heating of a flowing mixture of SiH_4, He, and H_2 to produce nonluminescent nanoparticles. These were etched with a mixture of HNO_3 and HF to reduce their size and passivate their surfaces. The particles were washed with water and methanol and finally collected by filtration. The resulting Si nanoparticles exhibit bright red or orange photoluminescence under UV excitation and have predominantly Si−H bonds on their surface.

Surface Pretreatment. The Si nanoparticles having predominantly Si−H bonds on their surface were first immersed in a "Piranha" solution (a mixture of 70 vol % concentrated sulfuric acid (98 wt %) and 30 vol % of a hydrogen peroxide solution (30 wt %)), sonicated for a few minutes and boiled for about 30−60 min to generate a high coverage of Si−OH groups on the surface of the nanoparticles. The particles were then washed with a large amount of distilled water and dried under vacuum for subsequent surface treatment.

Silane Treatment to Produce SAM. After the treatment by "Piranha" solution, the nanoparticles were placed into a solution of (3-bromopropyl)trichlorosilane in dried toluene (25 μL in 25 mL) under a nitrogen atmosphere, sonicated for 15 min, held at room temperature for 24 h, and then washed with dried toluene in an ultrasonic bath to remove the unreacted (3-bromopropyl)trichlorosilane. Finally, the particles were removed from the nitrogen atmosphere, collected by filtration, rinsed successively with toluene, acetone, and ethanol, and finally dried.

Aniline Functionalization and Graft Polymerization. The SAM silicon nanoparticles were immersed in aniline contained in a Pyrex tube for 48 h at room temperature. After the covalent substitution of the Br atoms of the SAM by aniline, the particles were washed with spectroscopic-grade methanol and then added to a 1 M HCl solution containing 0.1 M aniline and sonicated for 15 min. After that, a 0.1 M $(NH_4)_2S_2O_8$/1 M HCl solution was added and the mixture was allowed to polymerize in an ultrasonic bath for 30 min. In this step polyaniline was formed in its emeraldine (EM) salt state. The EM salt grafted on the nanoparticle surface was converted to the neutral EM base by adding a 0.1 M NaOH solution and then washing with a large amount of doubly distilled water. The surface-modified nanoparticles were subsequently washed several times in a large volume of NMP in order to remove any physically adsorbed EM base. Finally, the solution was centrifuged and the nanoparticles were obtained by filtration. The PANI−Si nanoparticles were washed with alcohol followed by deionized water to remove any residual NMP before being dried under reduced pressure.

(50) Huang, W. S.; MacDiarmid, A. G. *Polymer* **1993**, *34*, 1833.
(51) Sergeev, A.; Mitin, V.; Srtrocio, M. *Physica B* **2002**, *316*, 369.
(52) (a) Jordan, R.; West, N.; Ulman, A.; Chou, Y.-M.; Nuyken, O. *Macromolecules* **2001**, *34*, 1606. (b) Nuss, S.; Böttcher, H.; Wurm, H.; Hallensleben, M. L. *Angew. Chem., Int. Ed.* **2001**, *40*, 4016. (c) Mandal, T. K.; Fleming, M. S.; Walt, D. R. *Nano Lett.* **2002**, *2*, 3−7. (d) Weck, M.; Jackiw, J. J.; Rossi, R. R.; Weiss, P. S.; Grubbs, R. H. *J. Am. Chem. Soc.* **1999**, *121*, 4088.
(53) (a) Prucker, O.; Rühe, J. *Macromolecules* **1998**, *31*, 592. (b) Prucker, O.; Rühe, J. *Macromolecules* **1998**, *31*, 602.
(54) Li, Z. F.; Ruckenstein, E. *Macromolecules* **2002**, *35*, 9506.
(55) Ellis, J. R. *Handbook of Conductive Polymers*; Skotheim, T. A., Eds.; Marcel Dekker: New York, 1986; Vol. 1, p 505.

Scheme 1

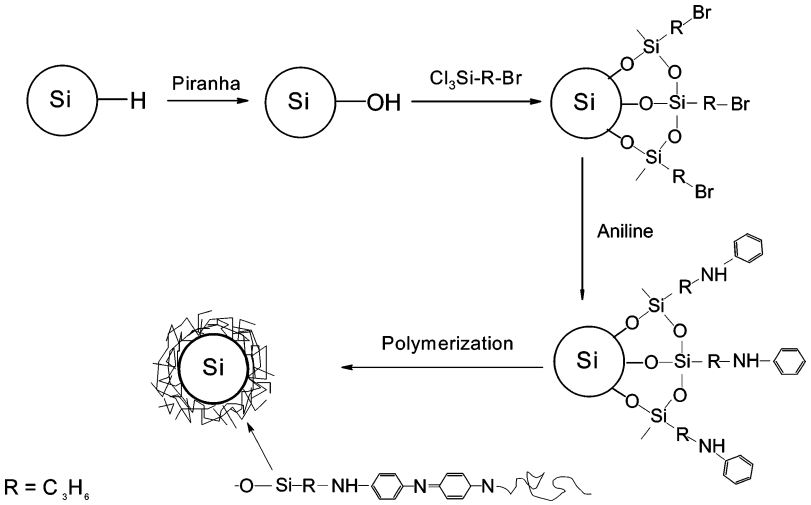

Characterization. XPS measurements were carried out on a Surface Science model SSX-100 Small Spot ESCA, possessing an Al Kα monochromatized X-ray source (1.48 keV photons). The pressure in the analysis chamber was maintained at 10^{-9} Torr or lower during the measurements. To compensate for surface charging, all binding energies were referenced to the C 1s hydrocarbon peak at 285 eV. In the peak analysis, the line widths (the width at half-maximum) of the Gaussian peaks were kept constant for the components of a particular spectrum. The surface elemental compositions were determined from the peak area ratios and were accurate to within 1%. The X-ray diffraction (XRD) patterns of the samples were obtained using a SIEMENS D500 diffractometer with Cu Kα radiation of 1.5406 Å wavelength. The diffraction data were recorded for 2θ angles from 15 to 60°, with a resolution of 0.02°. Transmission electron microscopy (TEM) investigations were carried out using a JEM-2010 electron microscope equipped with a tungsten gun operating at an accelerating voltage of 200 kV. Before the TEM measurements, the specimens were ultrasonically dispersed in methanol and dropped onto carbon-coated Cu grids. The Fourier transform infrared (FTIR) spectra were obtained using a Perkin-Elmer 1760 spectrometer with a resolution of 4 cm^{-1}. KBr pellets were employed for all the powders. Photoluminescence spectra were recorded with a SLM model 8100 spectrofluorimeter possessing a 420 nm emission cutoff filter. The excitation wavelength was set at 380 nm (for reasons discussed later). The average experimental error in determining the intensity of the PL was 7%. For time-resolved measurements, the PL was excited by ~300 fs pulses at a wavelength of 400 nm. These were generated by frequency doubling the 800 nm output from a Coherent RegA 9000 regenerative amplifier. The time-resolved photoluminescence (TRPL) data were collected and recorded using a spectrometer and a C4334 Hamamatsu streak camera.

The conductivity of the PANI−Si nanoparticles was determined by the four-probe method using compressed pellets and a Hewlett-Packard model 3478A digital multimeter. For each of the conductivities reported, at least three measurements were averaged. The electromagnetic shielding effectiveness (EMI SE) was determined over a frequency range from 10 to 1000 MHz using the coaxial cable method. The setup consisted of an Elgal (Israel) SET 19A shielding effectiveness tester with its input and output connected to a Hewlett-Packard (HP) 8510A network analyzer. An HP APC-7 calibration kit was used to calibrate the system. The EMI SE values expressed in decibels were calculated from the ratio of the incident to transmitted power of the electromagnetic wave using the equation

$$\mathrm{SE} = 10 \log([P_1/P_2]) \text{ (decibels, dB)}$$

where P_1 and P_2 are the incident power and the transmitted power, respectively.

Results and Discussion

The strategy for the grafting of PANI on the Si nanoparticles through the self-assembly (SAM) method is depicted in Scheme 1 and consists of the following steps: (1) the formation of Si−OH groups on the Si nanoparticle surface; (2) the formation of a well-defined SAM through the reaction of (3-bromopropyl)trichlorosilane with the hydroxyls of the Si−OH surface; (3) the debromination of this monolayer by substitution with aniline; and (4) the further reaction of the aniline sites with an aniline−oxidant solution to produce polyaniline grafted on the surface. Each step is discussed below in detail.

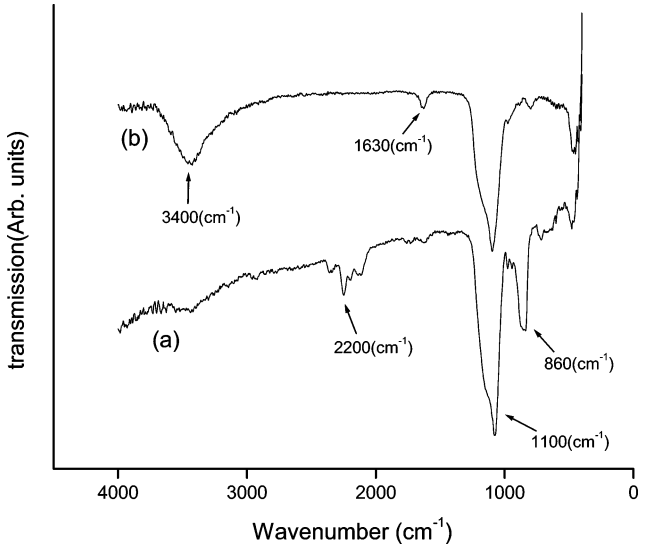

Figure 1. FTIR spectra of (a) freshly prepared Si nanoparticles that have Si−H on the surface (after HF treatment) and (b) Si nanoparticles bearing Si−OH on the surface after treatment with Piranha solution.

Formation of Si−OH on the Nanoparticle Surface. A freshly prepared Si nanoparticle surface is covered predominantly with hydrogen ($Si-H_x$) after etching with an HF/HNO_3 mixture and subsequent washing with 15% HF. To generate a well-defined functionalized surface by the method outlined in Scheme 1, a dense and uniform 3-bromopropylsilane monolayer must initially be formed, by a reproducible procedure, on the surface. For this reason, a highly hydroxylated surface was first generated by dispersing the particles in a boiling piranha solution for at least 30 min, but less than 1 h. Figure 1 presents the FTIR spectrum of the freshly prepared HF-etched Si nanoparticles before and after the treatment with piranha solution. Curve a in Figure 1 is a typical FTIR spectrum

of the freshly prepared Si nanoparticles. It displays the surface $Si-H_x$ ($x = 1-3$) stretching vibration modes around 2200 cm^{-1} and scissors vibration mode at 860 cm^{-1}. An absorption peak is also present at 1100 cm^{-1} due to the presence of surface silicon oxide (Si−O−Si bending vibrations) on the Si nanoparticles. Curve b in Figure 1 is the FTIR spectrum of the particles after treatment with piranha solution. Compared with that of the freshly prepared Si nanoparticle in curve a, both the Si−Hx stretching mode at 2200 cm^{-1} and scissors vibration mode at 860 cm^{-1} have disappeared and an intense Si−OH stretching mode at 3400 cm^{-1} and a bending mode at 1630 cm^{-1} have appeared.[56] The above results indicate that the Si−H bonds were replaced by Si−OH bonds in this step.

Formation of a Self-Assembled Bromopropylsilane Monolayer and further Surface Functionalization with Aniline. The Si nanoparticles with hydroxylated surfaces were exposed at room temperature, in a dry N_2 atmosphere, to a (3-bromopropyl)trichlorosilane solution in anhydrous toluene for about 24 h, during which the trichlorosilane groups of the (3-bromopropyl)trichlorosilane reacted with the hydroxyl groups of the Si nanoparticle surface. The particles were then rinsed with toluene, removed from the inert atmosphere, washed again with toluene, and sonicated in spectroscopic grade methanol. After being rinsed, the particles were left with uniformly dense (3-bromopropyl)silane films covalently linked to the surface. Parts a and b of Figure 2 present the wide scan XPS spectra of Si nanoparticles with hydroxylated surfaces and of particles covered by a self-assembled $-SiC_3H_6Br$ monolayer, respectively. The appearance of the Br and C peaks in Figure 2b indicates that $-SiC_3H_6Br$ was covalently bound to the silicon surface. The atomic ratio of C/Br is 3.2, which is consistent with the stoichiometry of bromopropylsilane. The silanized Si nanoparticles bearing $-SiC_3H_6Br$ monolayers were then placed in aniline at room temperature for 48 h. In this step the bromine atoms were substituted by aniline. Then the particles were rinsed with dried toluene, sonicated in spectroscopic grade methanol, and then dried. Figure 2c presents the wide scan XPS spectrum of these particles. Comparing parts b and c of Figure 2, one can see that the Br 3d signal of the $-SiC_3H_6Br$ (at 70.3 eV) from Figure 2b was replaced by a new N 1s signal in Figure 2c. The binding energy (BE) of N 1s, 399.3 eV, indicates that the signal is from an NH group covalently connected to a benzenyl ring. After reaction with aniline, the surface Br atom fraction obtained from the XPS measurements was reduced from 4.3% to 0.7%, which is within the ∼1% uncertainty of the XPS measurements of atomic composition. This indicates that the displacement of Br by aniline was nearly complete, though there may still be small peaks corresponding to Br in the spectrum of Figure 2c. These results show that a chemical substitution reaction occurred between aniline and −Br on the silane monolayer and that aniline was anchored to the silicon surface through a chemical bond.

The Graft Polymerization of Aniline on the Aniline−Silicon Surface. The graft oxidative polymerization of aniline was carried out via the conventional method, by introducing the aniline-primed Si nanoparticles in aniline/HCl aqueous solution for polymerization in an ultrasonic bath. Figure 3 presents the wide scan XPS and the N 1s core-level spectra of the silicon nanoparticles after the oxidative graft polymerization in a 1 M HCl solution containing 0.1 M aniline and 0.1 M ammonium persulfate. After polymerization, the surface-grafted polyaniline in the emeraldine (EM) salt state was converted to its neutral EM base form as described in the

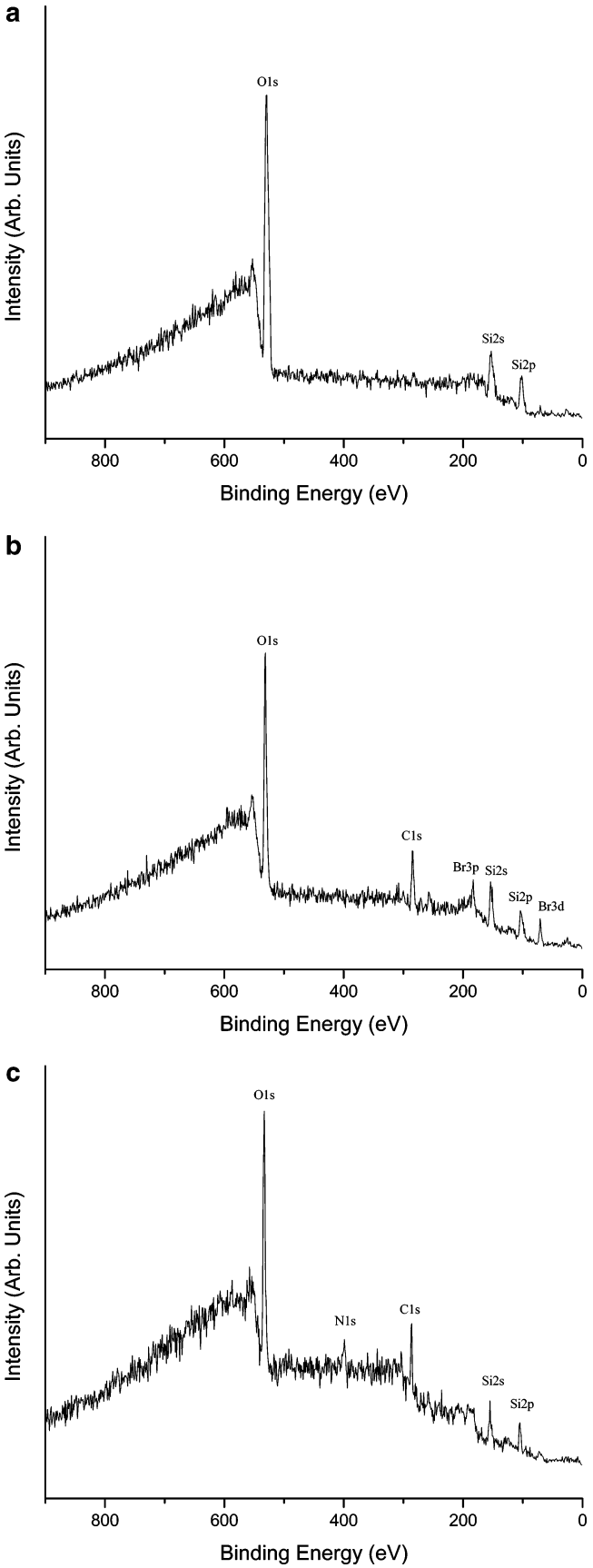

Figure 2. XPS wide scan spectra of silicon nanoparticles (a) after treatment with piranha solution, (b) after formation of the bromopropylsilane SAM, and (c) after substitution reaction of Br with aniline.

(56) Beckmann, K. H. *Surf. Sci.* **1965**, *3*, 314.

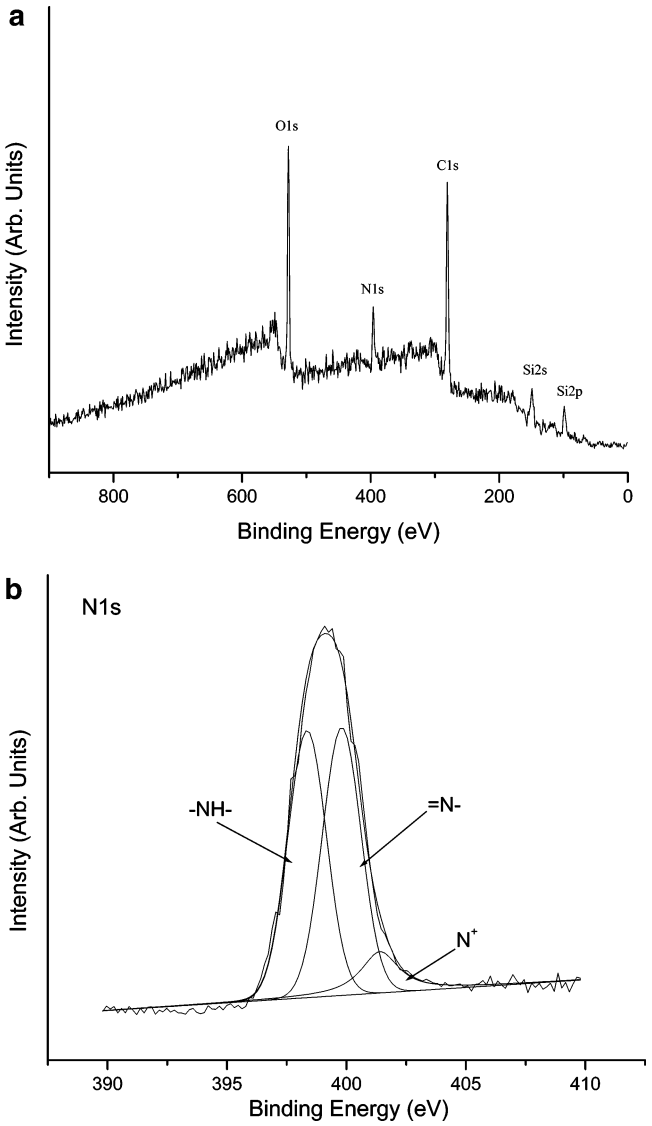

Figure 3. (a) XPS wide scan spectrum and (b) N 1s core-level spectrum of silicon nanoparticles grafted with PANI.

previous section. Compared with Figure 2c, the increase in the intensities of the N 1s and C 1s signals in the XPS wide scan spectrum of Figure 3a indicates that the oxidative graft polymerization of aniline, which brings carbon and nitrogen to the silicon surface, has taken place. The curve-fitted N 1s core-level spectrum of the PANI on the Si nanoparticles (Figure 3b) reveals the predominant presence of two types of structures corresponding to the binding energy (BE) peaks at 398.2 and 399.4 eV. These can be assigned to the quinonoid imine (═N−) and benzenoid amine (−NH−) structures, respectively. The almost equal proportions of the imine and amine nitrogen in the N 1s core-level spectrum of the particle surface are consistent with the EM base form ([═N−]/[−NH−] ratio ∼ 1) of PANI. The residual high binding energy tail (>400 eV) in the N 1s spectrum is probably due to some surface oxidation products, or a weakly charged-transfer complexed oxygen. The above N 1s spectrum is similar to that of the polyaniline homopolymer.[57] This confirms the successful grafting of the PANI to the surface of the Si nanoparticles.

The FTIR absorption spectra of PANI homopolymer powder and PANI grafted on the Si nanoparticles are

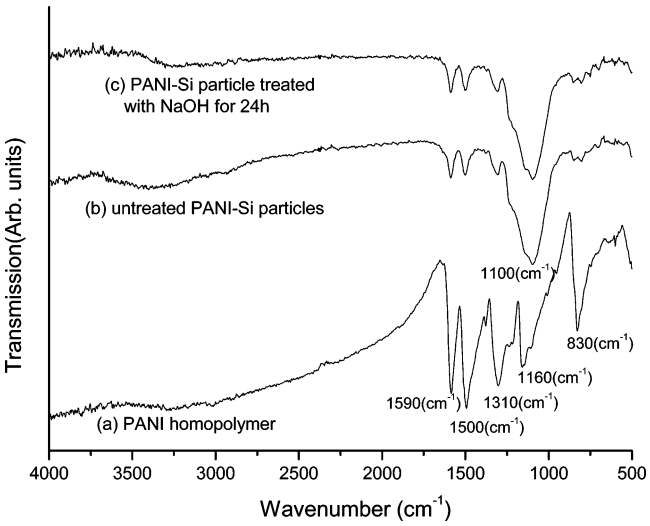

Figure 4. FTIR spectra of (a) EM base homopolymer, (b) PANI-capped Si nanoparticles, and (c) PANI-capped Si nanoparticles after immersion in 0.1 M NaOH for 24 h.

compared in Figure 4. For PANI homopolymer powders the main peaks at 1590 and 1500 cm^{-1} can be assigned to the stretching vibrations of quinone and benzene rings, respectively. The peak at 1310 cm^{-1} can be assigned to the C−N stretching vibration of a secondary aromatic amine. The peak at 1160 cm^{-1} corresponds to the aromatic C−H in-plane bending mode. The out-of-plane bending of C−H in the 1,4-disubstituted benzene ring is reflected in the 830 cm^{-1} peak. The similarity between the PANI grafted on the Si nanoparticles and the PANI homopolymer powder further confirms that PANI was successfully grafted on the surface of the Si nanoparticles. In addition, the PANI-capped Si nanocomposites exhibit a strong peak at 1100 cm^{-1}, which can be attributed to Si−O−Si at the Si/PANI interface. Finally, as shown by Figure 4, after the PANI-capped Si nanoparticles were immersed in a 0.1 M NaOH solution for 24 h, the FTIR of the sample showed no change in the spectrum. This shows that PANI grafted on the Si particles surface was stable under these conditions and can protect the Si particles from degradation by basic solutions (vide infra).

XRD Analysis. The crystallinity of Si nanoparticles after grafting of PANI on their surface was also investigated. Figure 5 presents the XRD patterns of the freshly prepared Si nanoparticles and of PANI-coated particles. Before the PANI coating, there are three main sharp peaks at 2θ = 28.1°, 47.4°, and 56.2° (Figure 5a), which are characteristic of crystalline silicon.[34] These three main peaks are still present after the graft polymerization of PANI on the particle surface (Figure 5b), but an additional broad amorphous peak is present around 20°. The additional peak corresponds to the XRD pattern of PANI and is similar to the PANI XRD results reported previously.[58] The presence of the three crystalline Si peaks and the persistence of the photoluminescence of the PANI coated Si nanoparticles, vide infra, confirm that the graft polymerization of PANI did not affect the crystallinity of the Si nanoparticles. The inset in Figure 5 shows the 2θ = 47.4° peak for both samples, normalized and overlaid for comparison. For the PANI-coated particles, the peak is slightly broader, possibly indicating a slight decrease in crystal size. However, peak broadening is also affected by strain, and it is reasonable to expect that the SAM formation and PANI coating would change the strain state

(57) Li, Z. F.; Kang, E. T.; Neoh, K. G.; Tan, K. L. *Synth. Met.* **1997**, *87*, 45.

(58) Chen, S. A.; Lee, H. T. *Macromolecules* **1993**, *26*, 3254.

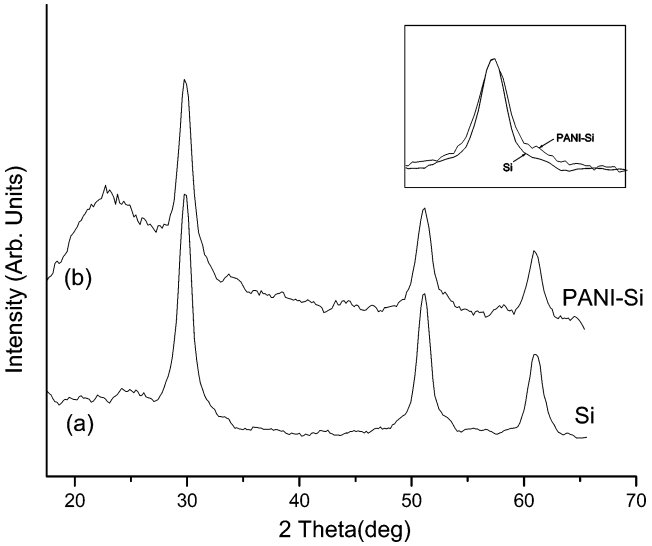

Figure 5. XRD patterns of (a) freshly prepared Si nanoparticles after etching and (b) PANI-capped Si nanoparticles. The inset shows the $2\theta = 47.4°$ peak for both samples, overlaid for comparison of the peak width.

of the particles. Thus, one cannot conclude, based on the slight XRD peak broadening alone, that there is any significant decrease in particle size during the coating process.

TEM. Samples of uncapped and PANI-capped Si nanoparticles were dispersed and sonicated in methanol. The dispersion was dropped onto holey carbon-coated Cu TEM grids and then dried at room temperature. Panels a and b of Figure 6 present micrographs of uncapped and PANI-capped Si nanoparticles, respectively. Figure 6a shows that the uncapped particles are not well dispersed and that they aggregated significantly during solvent evaporation from the TEM grid. However, one can still observe (in Figure 6a) that most of the Si nanoparticles were in the range of 3−5 nm.[59] For the PANI-capped Si nanoparticles in Figure 6b, the dispersibility of the nanoparticles was slightly improved and one can observe that most of the particles have diameters in the range of 8−10 nm. The core−shell structure observed in Figure 6b indicates that the PANI coating was around 2−3 nm thick.

Photoluminescence and Stability of the PANI−Si Nanoparticles. Neither the hydrogen surface termination of freshly etched silicon particles nor the thin oxide that forms upon exposure of these particles to air for a few hours protects the particles from quenching of their photoluminescence by molecules in solution. This restricts the potential use of Si nanoparticles in the fabrication of devices. In our experiments, it was found that the PL of freshly prepared Si nanoparticles was quenched on a time scale of seconds to minutes after immersion in ammonium hydroxide or other basic solutions and by many nitrogen-containing organic solvents such as NMP and amines. Quenching of silicon nanocrystal luminescence by amines is a well-known phenomenon.[60] The PL stability of the PANI-capped Si nanoparticles was examined and compared with that of the freshly prepared Si nanoparticles after their immersion in a series of acidic or basic solutions and various organic solvents. We found that the PANI-capped Si nanoparticles maintained their PL even after immersion in NH_4OH or NaOH solutions, hexylamine, or NMP for 24 h. In contrast, the PL of the uncapped Si nanoparticles was quickly quenched after their immersion in the above solutions and solvents. Table 1 summarizes quantitatively the PL change of the freshly prepared Si nanoparticles, of those that had been silanized but not coated with PANI, and of PANI-capped silanized Si nanoparticles after their immersion in various chemical environments for 24 h. One can see that the PL stability of Si nanoparticles was greatly improved after their silanization by the self-assembly method. These results suggest that the coverage of the nanoparticle surface by a dense bromopropylsilane SAM stabilizes the PL by preventing intimate contact between quenching molecules and the Si nanoparticle surface. It seems that there is no

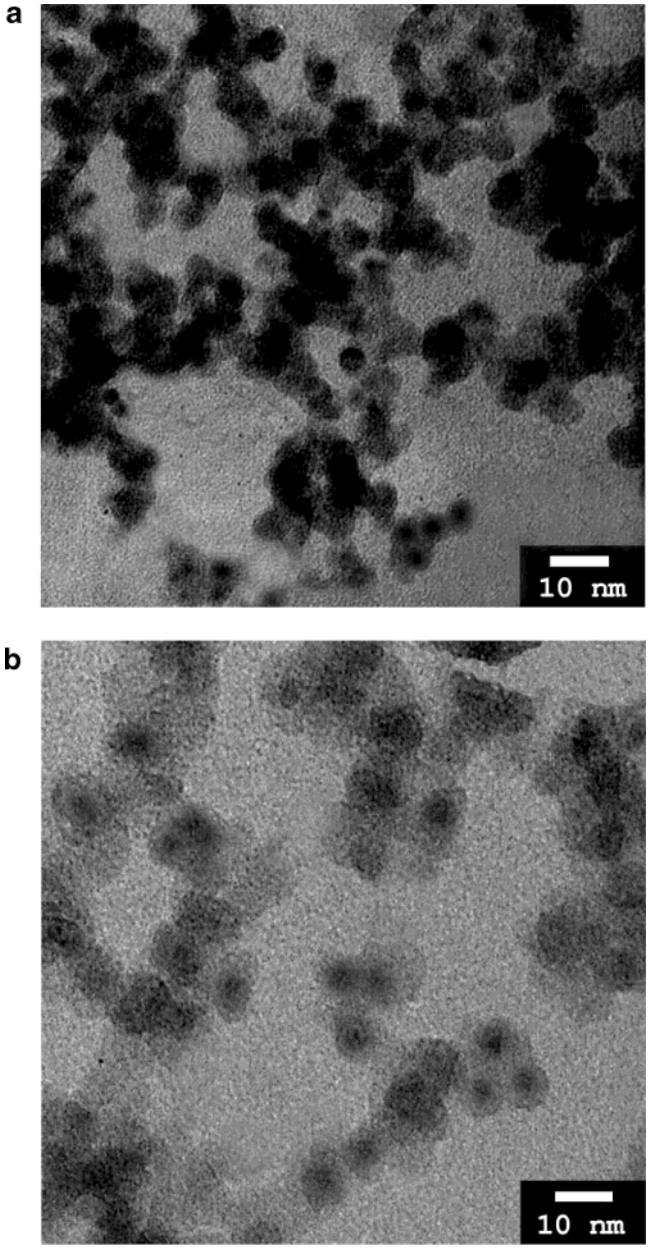

Figure 6. Transmission electron micrographs of (a) uncapped Si nanoparticles and (b) PANI-capped Si nanoparticles.

(59) Covalent attachment of other small organic molecules (octadecene, undecylenic acid, octadecyltrimethoxysilane) to the silicon nanoparticles allows them to form stable dispersions in a variety of nonpolar and semipolar solvents. These well-dispersed particles do not agglomerate during solvent evaporation when cast on a TEM grid. For those particles, high-resolution TEM imaging clearly shows individual silicon nanoparticles 3−5 nm in diameter. Details of this will be presented in a separate manuscript (Li, X.; He, Y.; Swihart, M. T. Submitted to *Langmuir*).

(60) Harper, J.; Sailor, M. J. *Langmuir* **1997**, *13*, 4652.

Table 1. Percentage Change of the Photoluminescence Intensity of Si and Modified Si Nanoparticles after Their Immersion in Different Chemical Solutions for 24 h[a]

nanoparticles	0.1 M HCl	0.1 M NaOH	0.1 M NH_4OH	NMP	hexylamine
Si	120[b]	20	0	0	0
silane−Si	100	75	65	78	82
PANI−silane−Si	100	75	70	95	93

[a] Percentage given is 100 times the ratio of the peak PL intensity after 24 h to that immediately after dispersion into the solution or solvent. [b] The PL intensity increased for uncapped Si particles after its immersion in 0.1 M HCl and a blue shift by about 15 nm occurred.

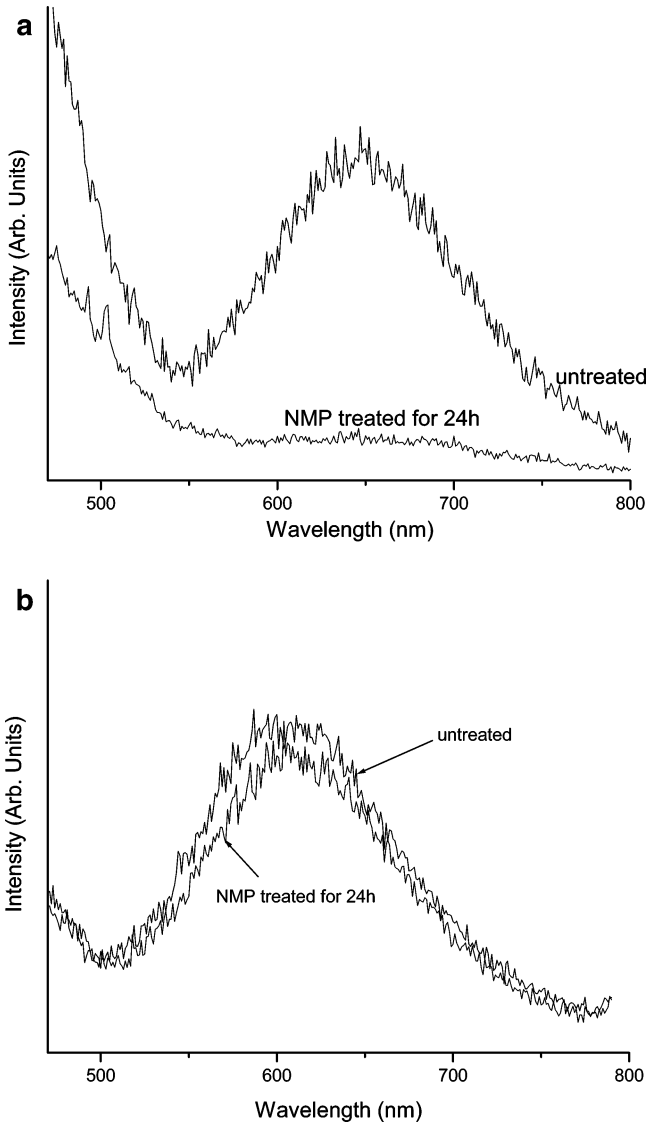

Figure 7. Normalized photoluminescence spectra of (a) freshly prepared Si nanoparticles before and after immersion in NMP solution for 24 h and (b) PANI-capped Si nanoparticles before and after immersion in NMP solution for 24 h.

dramatic effect of the conductivity of PANI on the PL intensity and stability since the PANI-coated Si particles behave in the same way as silane-coated particles in acidic solutions (where PANI is protonated and conductive) and basic solutions (where PANI is in its relatively nonconductive emeraldine base form). However, the PANI-coated SAM layer has made the nanoparticles much more robust toward nitrogen-containing organic solvents such as NMP and hexylamine. As a more detailed example, Figure 7 presents the PL spectra of the PANI-capped Si nanoparticles and uncapped Si nanoparticles before and after immersion in NMP for 24 h. Comparing parts a and b, one can see that the PL stability was enhanced greatly by capping with PANI. For PANI-capped Si nanoparticles, the PL intensity decreased slightly after 24 h in NMP, but for the uncapped particles the PL disappeared completely. It should be noted that before immersing in NMP the absolute PL intensity was lower from the coated particles than the uncoated particles due to some absorption by PANI of both the UV light used to excite the PL and the visible light emitted by the nanoparticles. The UV absorption spectrum of both the PANI-coated particles and PANI homopolymer has a peak at 300 nm and is relatively large and constant for wavelengths larger than 600 nm. We selected in our experiments an excitation wavelength of 380 nm, for which the absorption by PANI is relatively low. The PL emission was in the wavelength range of 620−670 nm, where there is significant absorption by the PANI coating.

Comparing parts a and b of Figure 7, one sees that the PL peak was blue-shifted by about 40 nm for the PANI-capped Si nanoparticles compared to the uncapped particles. Further investigation showed that this blue shift occurs during the pirhanha treatment and formation of the bromopropylsilane SAM, and not during the graft polymerization of the PANI. Thus, it is not an effect related to the conductivity of PANI, but simply to changes in the particle surface when Si−H termination is replaced by Si−O−H linkages. If the PL is a result of recombination of quantum-confined carriers in the nanoparticle core, then a blue shift should indicate a reduction in particle size or greater confinement at the surface. If some of the PL arises from recombination at the surface, then changing the surface termination will directly change the energy of these surface states (or remove them). Decreased recombination via surface states would also appear as a blue shift. On the basis of the TEM images and XRD peak broadening discussed above, it does not appear that there is a significant decrease in particle size, but there may be some small decrease. In previous work[34] on uncapped particles, there was a clear increase in XRD peak width with decreasing peak PL wavelength for comparable changes in PL wavelength. Thus, it seems likely that the blue shift is related to changes at the Si nanocrystal surface rather than to a decrease in the nanocrystal size.

The fact that the polyaniline coating has little or no effect on the PL spectrum suggests that the charge carriers responsible for the PL remain confined in the Si nanoparticle core and there is no transport of holes (positive charge carriers) into the PANI coating. The blue shift of the PL between spectra a and b of Figure 7 occurs during the pirhanha etch and silanization and there is essentially no further shift in the PL spectrum after coating with PANI. A few time-resolved PL measurements were also performed after coating, and these showed no significant change in the PL lifetimes. No new fast recombination pathways were observed, even with the picosecond time resolution of these experiments. The PL lifetimes are of the order of tens of microseconds for both the untreated and PANI-capped particles. If new recombination pathways (radiative or nonradiative) had been introduced due to transport of charge carriers into the polyaniline, a change in PL lifetime would have been expected. Thus, the PL mechanism is apparently the same in the treated and untreated particles, and there is no indication of any transport of holes into the PANI or creation of any new radiative or nonradiative paths involving the PANI coating or Si/PANI interface. From the point of view of the Si nanoparticle, the PANI coating acts as an insulator, and charge carriers remain confined in the particle. This is

perhaps interesting, because from an "external" point of view, the PANI is quite a good conductor, as detailed below. Apparently, either the work function of PANI is sufficiently high that holes generated in the Si nanoparticle cannot leave the particle or the propylsilane linking groups at the interface provide a sufficient barrier to prevent carrier transport from the silicon to the PANI.

Conductivity and Electromagnetic Shielding Properties. The electrical conductivity of pellets pressed from the doped PANI-capped Si nanoparticles was as high as 2.7×10^{-2} S/cm, which is 6 orders of magnitude larger than that of pellets pressed from the freshly prepared Si nanoparticles($\sim 10^{-8}$ S/cm). The relatively high conductivity rendered by PANI can provide the Si/PANI nanoparticles and nanocomposites prepared from them with good electrostatic dissipation and electromagnetic interference shielding properties. Figure 8 provides information about the electromagnetic shielding of PANI-capped Si nanoparticles. The EMI shielding effectiveness (SE) measurements were carried out using the coaxial transmission line method in the frequency range of 10−1000 MHz. Figure 8 indicates that the SE at high frequencies is around 11 dB, and at lower frequencies it is larger than 18 dB. For the freshly prepared Si nanoparticles without capping by PANI, the SE value is around zero; there is no EMI shielding effect.

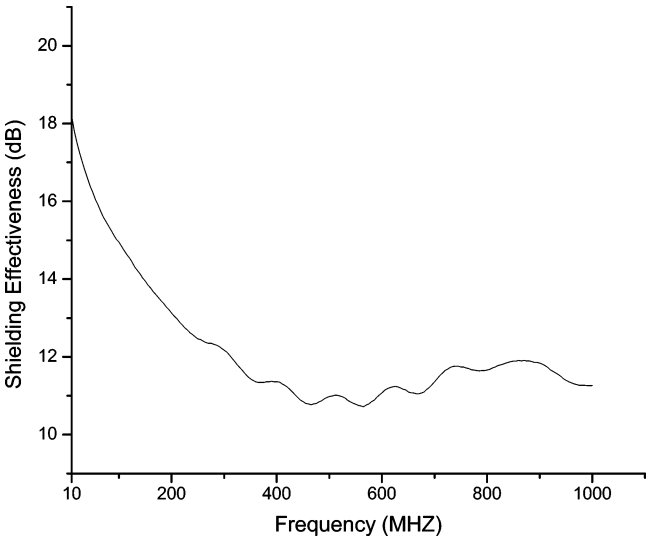

Figure 8. The electromagnetic shielding effectiveness of PANI-capped Si nanoparticles.

Conclusion

Free-standing luminescent crystalline Si nanoparticles were successfully capped with polyaniline through reaction with a self-assembled bromopropylsilane monolayer. The composition, structure, morphology, and other physical properties of the PANI-capped Si nanoparticles were examined by X-ray photoelectron spectroscopy, Fourier transform infrared spectroscopy, and X-ray diffraction, which proved that polyaniline was grafted onto the surface without affecting the crystallinity of the silicon nanoparticles. The bromopropylsilane SAM and PANI coating greatly stabilized the PL of the Si nanoparticles against quenching and degradation and allowed the particles to retain their PL after treatment with basic solutions, amines, or NMP, all of which quench or degrade the PL of the uncoated particles. The PL spectrum and lifetimes were not affected by the presence of the conductive PANI coating, indicating that charge carriers are not transported from the silicon core to the PANI shell. The electrical conductivity of PANI-capped Si nanocomposites formed by pressing the coated nanoparticles into pellets reached 2.7×10^{-2} S/cm.

Acknowledgment. We are grateful to Xuegeng Li and Yuanqing He for producing the unetched Si nanoparticles, and to W. D. Kirkey for help with photoluminescence measurements.

LA0358926